Wind and Structures, *Vol. 28, No. 4 (2019) 239-253*
DOI: https://doi.org/10.12989/was.2019.28.4.239

Wind field simulation over complex terrain under different inflow wind directions

Wenfeng Huang* and Xibin Zhang

School of Civil Engineering, Hefei University of Technology, Hefei, 230009, China

(Received March 13, 2018, Revised September 9, 2018, Accepted October 11, 2018)

Abstract. Accurate numerical simulation of wind field over complex terrain is an important prerequisite for wind resource assessment. In this study, numerical simulation of wind field over complex terrain was further carried out by taking the complex terrain around Siu Ho Wan station in Hong Kong as an example. By artificially expanding the original digital model data, Gambit and ICEM CFD software were used to create high-precision complex terrain model with high-quality meshing. The equilibrium atmospheric boundary layer simulation based on RANS turbulence model was carried out in a flat terrain domain, and the approximate inflow boundary conditions for the wind field simulation over complex terrain were established. Based on this, numerical simulations of wind field over complex terrain under different inflow wind directions were carried out. The numerical results were compared with the wind tunnel test and field measurement data for land and sea fetches. The results show that the numerical results are in good agreement with the wind tunnel data and the field measurement data which can verify the accuracy and reliability of the numerical simulation. The near ground wind field over complex terrain is complex and affected obviously by the terrain, and the wind field characteristics should be fully understood by numerical simulation when carrying out engineering application on it.

Keywords: complex terrain; RANS turbulence model; CFD simulation; equilibrium atmospheric boundary layer; comparison

1. Introduction

The research on the wind field over complex terrain includes three methods: field measurement, wind tunnel test and numerical simulation. Field measurement can obtain the detail wind field information for the specific site, but it cannot provide the wind field characteristics for the entire region. Wind tunnel test is a commonly used method to simulate the wind field over complex terrain. However, the test cycle of wind tunnel test is longer and the cost is higher. In addition, for a large area of complex terrain, the wind tunnel test requires a smaller scale model which creates some difficulties and the accuracy of the test is yet to be discussed. Computational fluid dynamics (CFD) simulation is attracting more attentions due to its advantages of digitalization, full size, high precision, short simulation period and low cost (Salmon *et al.* 1988, Bitsuamlak *et al.* 2004, Burlando *et al.* 2007, Kikuchi and Ishihara 2012, Li *et al.* 2013, Marjanovic *et al.* 2014, Castellani *et al.* 2017, Dhunny *et al.* 2017).

Many researchers have carried out the numerical simulation of wind field over complex terrain. Uchida and Ohya (1999) used digital elevation data to simulate the mountain topography and studied the wind field over complex terrain. Kim *et al.* (2000) used the Reynolds Average Navier-Stokes (RANS) method to simulate the wind field over hilly terrain and obtained a better simulation result of the RNG k-ε turbulence model than the standard k-ε model. Ishihara (2003) built additional buffer zones around the complex terrain to simulate the real complex terrain and the numerical results were close to the wind tunnel test. Bitsuamlak *et al.* (2004) simulated wind fields over simple 2D and 3D terrain and found that the numerical results of the windward surface tend to be closer to the observed data than the lee side. Hui *et al.* (2006) conducted a comparative study of wind tunnel test and CFD simulation for wind field over complex mountain and showed that RANS and LES were in good agreement with wind tunnel test data. Lee *et al.* (2010) studied the distribution of wind field around a wind power plant in a complex mountainous through three-dimensional wind field simulation. Petry *et al.* (2012) conducted a comparative analysis of wind tunnel test and numerical simulation of wind field over complex terrain, and found that, compared with k-ε turbulent model, the SST k-ω model was in good agreement with the experimental results. Abdi and Bitsuamlak (2014) used a variety of turbulence models to simulate wind fields over complex mountainous and found that the RANS turbulence model is better for leeward turbulence due to the negative pressure gradients. Blocken *et al.* (2015) compared the field measurements and numerical simulations of wind field over complex terrain. The results showed that the realizable k-ε model could accurately estimate the complex flow in the mean wind field and the funnel effect in wind field over complex terrain. Liu *et al.* (2016) used LES model to simulate wind fields over different types of terrain and achieved the same results as the experiment. Li *et al.* (2017) studied the influence of inlet boundary conditions on mountainous wind environment. Dhunny *et al.* (2017)

*Corresponding author, Associate Professor
E-mail: wfhuang@hfut.edu.cn

http://www.techno-press.com/journals/was&subpage=7 ISSN: 1226-6116 (Print), 1598-6225 (Online)

studied the key parameters of the numerical simulation and used the best method to simulate the wind field over the highly complex topography to obtain satisfactory results. Risan *et al.* (2018) studied the performance of the hybrid model of RANS and LES under highly complex topography.

The basis for the successful numerical simulation of wind field over complex terrain lies in the establishment of an accurate complex terrain model with high-quality meshing and the use of suitable inflow boundary conditions. The complex terrain model usually restores the topographic features of the terrain by means of digital terrain information (Uchida and Ohya 1999, Sherman 1978, Weng *et al.* 2000, Uchida and Ohya 2008, Kuo *et al.* 2016). However, the elevation difference at the edge of the complex terrain model has great impact on the wind field and has not caused enough attention of the researchers. Some even do not do any processing on the edge of the terrain so that the simulation results have lower credibility. In terms of meshing (Scargiali *et al.* 2005, Garcia and Boulanger 2006, Meo *et al.* 2008, Palma *et al.* 2008, Hussein and El-Shishiny 2009, Van Hooff and Blocken 2010, Li *et al.* 2016), due to the large research area of complex terrain models and considering the limitation of the grid numbers by computing resources, it is easy to cause the grid scale to be too large to accurately capture the detailed features of the flow field. In addition, because of the complexity of the terrain, the quality of the meshing is also variable. Equilibrium atmospheric boundary layer simulation is an important prerequisite for numerical simulation accuracy, but it is also easily ignored by many researchers. At present, the CFD models used in numerical simulation mainly include LES model (Liu *et al.* 2016, Uchida and Ohya 2003, Kamio *et al.* 2014, Conan *et al.* 2015, Chaudhari *et al.* 2017, Ma and Liu 2017) and RANS model (Kim *et al.* 2000, Hui *et al.* 2006, Petry *et al.* 2012, Abdi and Bitsuamlak 2014, Li *et al.* 2017, Li *et al.* 2006, Prospathopoulos *et al.* 2012, Murali and Rajagopalan 2017). However, the LES model has high requirements for grid quality and computer performance, and the applicability of wind field simulation over complex terrain needs further study. Because of the lower grid and computational requirements, RANS model is more suitable for the wind field simulation over complex terrain.

Based on a review of wind field simulation over complex terrain, it can be concluded that, few wind field simulations over complex terrain have considered the problems of the elevation difference at the edge of the complex terrain model, the meshing of the complex terrain model and the suitable inflow boundary conditions together. To simulate the wind field simulation over complex terrain more accurately, it is crucial to consider all these aspects together in the specific simulation. To fill such a gap, by taking the complex terrain around the Siu Ho Wan (SHW) station in Hong Kong as a case study, the expanded complex terrain model, high quality meshing grid and equilibrium atmospheric boundary layer simulation with approximate inflow boundary conditions are performed in this study. In detail, Gambit and ICEM CFD software are used to artificially expand the digital terrain data to build high precision complex terrain model with high-quality meshing. The inflow boundary conditions for wind field simulation over complex terrain are obtained by carrying out the equilibrium atmospheric boundary layer simulation based on RANS model. Finally, wind field simulations over complex terrain under different inflow wind directions are carried out. The simulated results are compared with wind tunnel test and field measurement data to verify the validity and reliability of the present numerical simulation method used in this paper.

2. Numerical simulations

2.1 Complex terrain model and mesh scheme

The SHW station is located at 22°18'21"N, 113°58'45"E. It is surrounded by a complex terrain as shown in Fig.1, and its digital terrain is shown in Fig. 2. The study takes the SHW station as the center and selects digital complex terrain data within a radius of 5 km. In order to solve the problem of inconsistent elevation at the selected complex terrain boundary, Eq. (1) is used to expand the original terrain to a flat terrain with zero elevation (Liu *et al.* 2016). The expanded terrain is shown in Fig. 3 and the blue part in Fig. 3(a) shows the expanded area between the original terrain and the zero-elevation plane. Then, the complex terrain model around the SHW station with a size of 22.14 km × 127.16 km × 5 km ($x \times y \times z$) is further established by combining Gambit and ICEM CFD software as shown in Fig. 4. The blocking ratio of the model is about 2.53% and meets the usual 3% requirement (Yamaguchi *et al.* 2006).

$$z_n(x,y)=\begin{cases} 0 & 2000+R<\sqrt{\left(x^2+y^2\right)} \\ z_e(x,y)\cdot\left[1-\dfrac{\sqrt{\left(x^2+y^2\right)}-R}{2000}\right] & R<\sqrt{\left(x^2+y^2\right)}\le 2000+R \\ z_e(x,y) & 0\le\sqrt{\left(x^2+y^2\right)}\le R \end{cases} \quad (1)$$

where $z_n(x,y)$, $z_e(x,y)$ are the expanded and the original terrain evaluation, respectively; R is the radius of complex terrain

Fig. 1 Topography around the SHW station

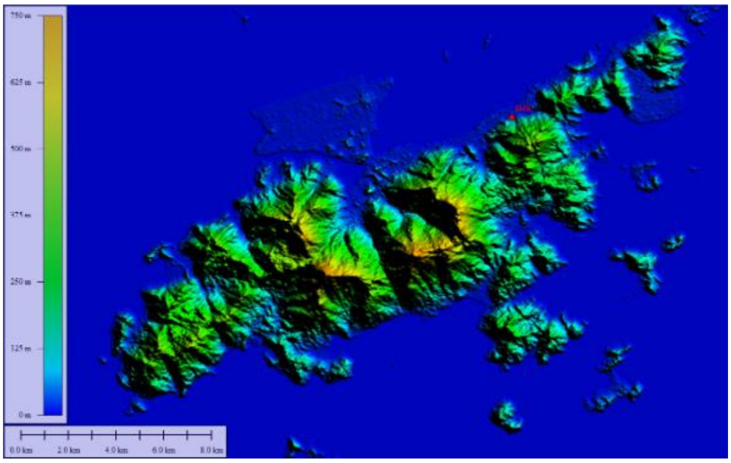

Fig. 2 Digital topography around the SHW station

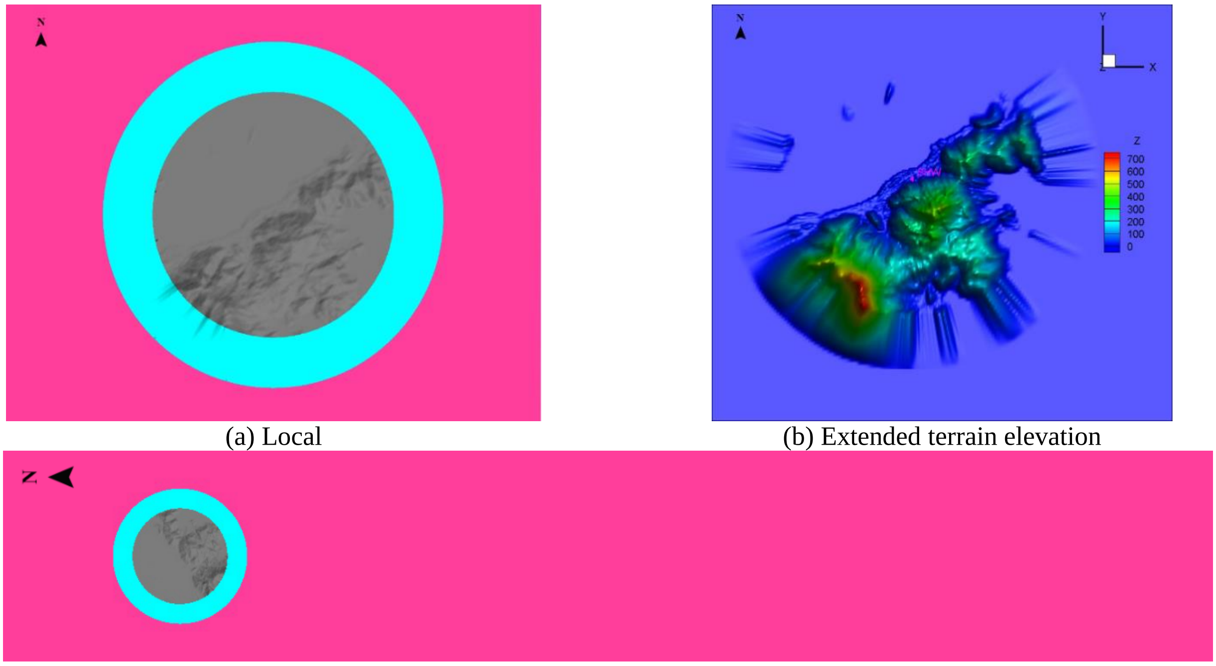

(a) Local (b) Extended terrain elevation

(c) Overall

Fig. 3 Extended local and overall complex terrain

The hexahedron structured grid of ICEM CFD was used in grid meshing of the computational domain. In order to achieve the purpose of saving computing resources and ensuring the accuracy of simulation results. The mesh independent test is performed by setting multiple sets of meshes with different degrees of mesh density. When the accuracy of the simulation results is basically unchanged, the mesh with appropriate mesh resolution is used in the final CFD simulation. In this study, three schemes of meshes are used to verify the mesh independence and shown in Table 1.

Mean wind speed profiles at the SHW station obtained from three meshing schemes for 0° inflow wind direction are shown in Fig. 5. The simulation results under three meshing schemes are basically the same, especially away from the ground surface. The simulation error appears mainly near the ground surface below 60 m height, in which the simulation error between scheme 1 and scheme 2 is less than 10% and the simulation error between scheme 2 and scheme 3 is less than 15%. Considering the current computing power and simulation accuracy, meshing scheme 2 is used in the final CFD simulation. The detail information about meshing scheme 2 is determined as follows: taking the SHW station as the center, the grid resolution within 1000 m along and perpendicular to the flow direction is 20 m, and the outward growth rate is 1.1, the maximum grid size is 40 m in the 4000 m range, the maximum grid size at the edge of the complex terrain is 100 m, the grids of inlet and side boundaries are increased to 200 m, the grids of outlet boundary increase to 300 m. In

Table 1 Meshing schemes

Meshing scheme	Numbers of cells (million)	Grid size within a certain range of the SHW (m)			Initial height (m)
		1000	4000	7000	
1	15.587	15	30	80	1
2	11.086	20	40	100	5
3	6.596	30	50	150	8

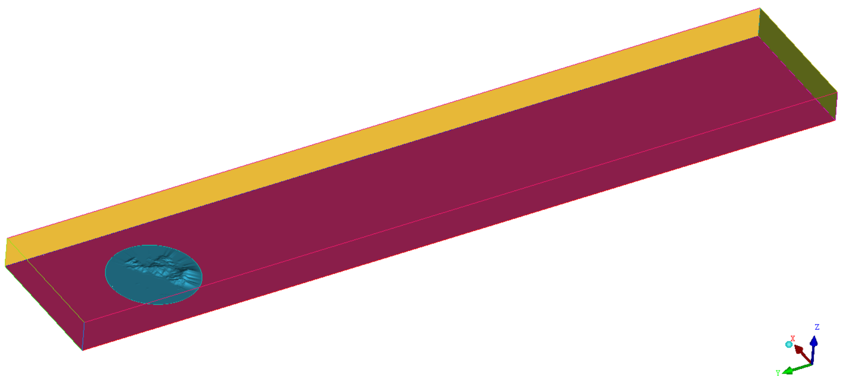

Fig. 4 Three-dimensional computational domain of complex terrain

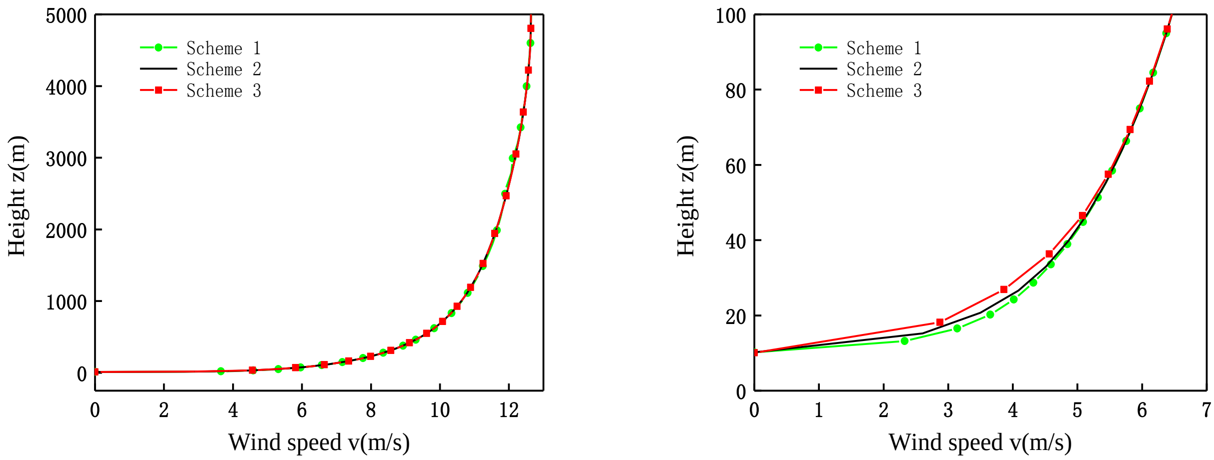

(a) Full height (b) Below 100 m height

Fig. 5 Mean wind speed profiles for 0° infow wind direction at the SHW station

vertical direction, the grid height of the first layer is 5 m, the growth rate is 1.08, and the resolution of the top grid is 200 m. The total number of grids is about 11,086,000. The grid of complex terrain computational domain is shown in Fig. 6 which has good texture mesh. As shown in Fig. 7, the minimum value of grid quality for the computational domain is 0.569, the maximum value is 1, of which 98.88% is greater than 0.9, which has good meshing quality and meets the calculation requirements.

2.2 Boundary conditions and solver algorithm

The equilibrium atmospheric boundary layer conditions derived from SST *k*-*ω* model include three aspects: mean wind speed, turbulent kinetic energy and specific dissipation rate, which can be expressed as follows

$$U_z = U_r \times \left(\frac{z}{z_r}\right)^{\alpha} \tag{2}$$

(a) Overall

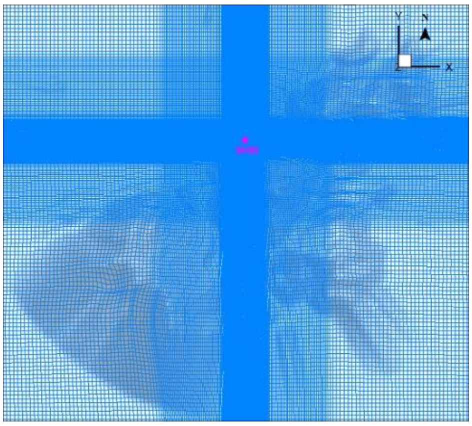

(b) Complex terrain

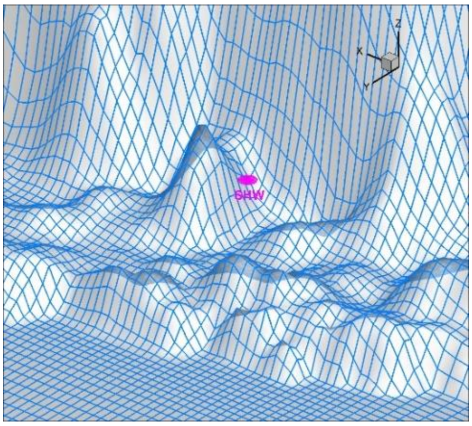

(c) The SHW station

Fig. 6 Mesh of complex terrain model

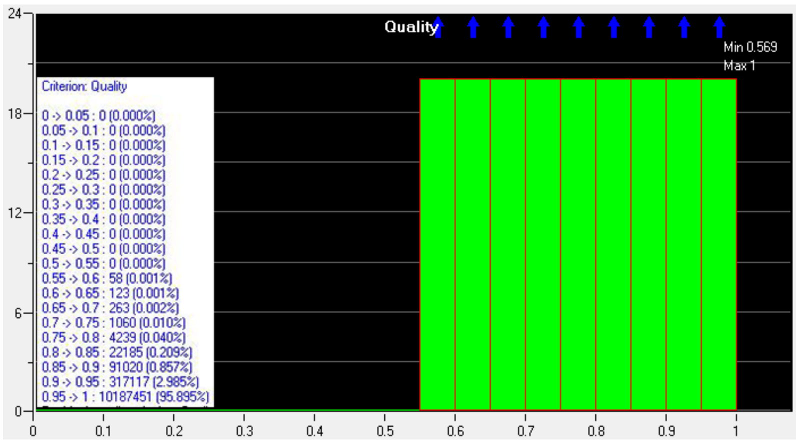

Fig. 7 Mesh quality of the complex terrain model

$$k = \sqrt{\frac{C_1}{\alpha} z^{\alpha} + C_2} \tag{3}$$

$$\omega = \frac{\alpha}{\sqrt{\beta^*}} \frac{U_r}{z_r^{\alpha}} z^{\alpha-1} \tag{4}$$

where U_z and U_r are the mean wind speeds at z and z_r heights; k is the turbulent kinetic energy; ω is the turbulent dissipation rate; α is the surface roughness index; C_1 and C_2 are constants; β^* is the model constant.

The wind speed profile and turbulence intensity profile associated with the study were obtained from wind tunnel test as shown in Figs. 8(a) and 8(b). In order to obtain C_1 and C_2 parameters shown in Eq. (3), values of turbulent kinetic energy k is obtained with the empirical expression $1.5(I_zU_z)^2$ as shown in Fig. 8(c). The fitting results of mean wind speed, turbulence intensity and turbulent kinetic

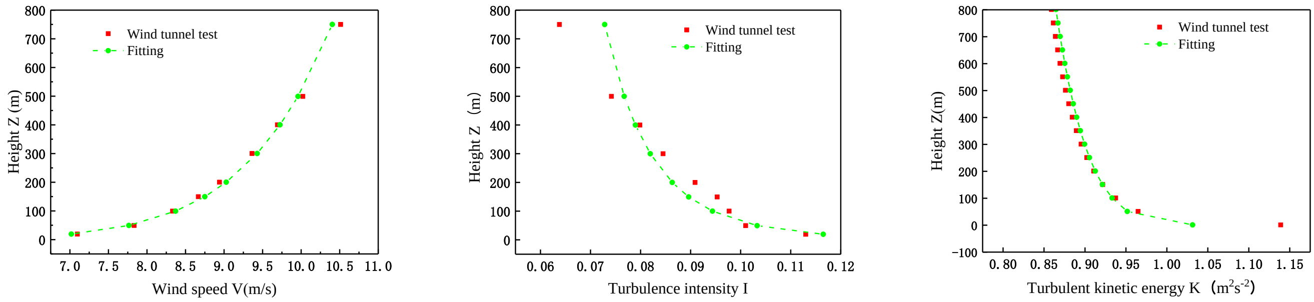

(a) Mean wind speed profile (b) Turbulence intensity profile (c) Turbulent kinetic energy

Fig. 8 Inlet boundary conditions

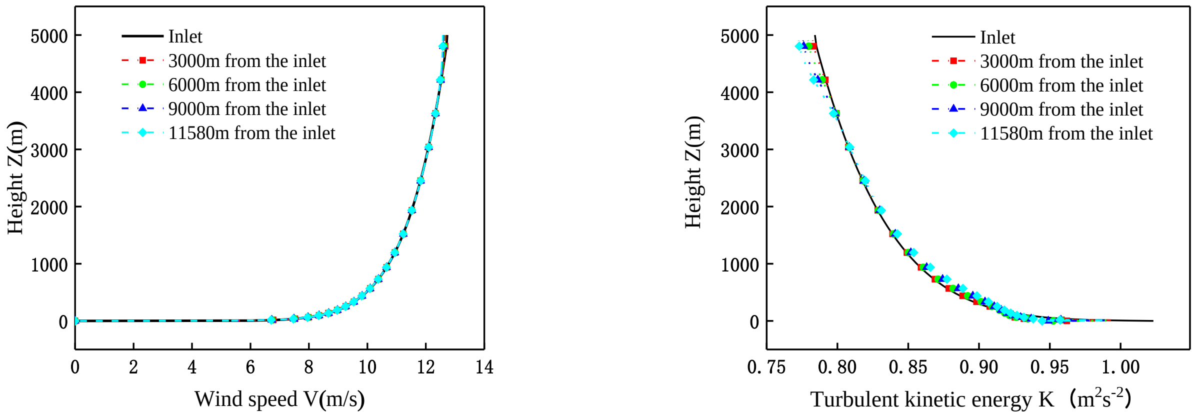

(a) Mean wind speed (b) Turbulent kinetic energy

Fig. 9 Mean wind speed and turbulent kinetci energy profiles for the empty domain

energy are shown in Fig. 8 with goodness of fit 0.994, 0.887 and 0.969, respectively.

The fitted values of the parameters are: U_r=8.28513, α=0.10745, C_1=-0.03234, C_2=1.36487. In addition, the optimal value of β^* is 0.02. The roughness height k_s used in the simulation is taken as 0.2 m.

Present CFD simulation has been performed with Fluent 18.2, which is a general-purpose code for fluid dynamic simulations produced by Fluent Inc. The surface of the topographic model is modeled as a non-slip wall boundary. The flow inlet boundary is set as equilibrium atmospheric boundary layer conditions with Eqs. (2)-(4) while the outlet boundary is specified as outflow boundary condition. The side and top boundaries are all defined in such a way that the gradients of flow variables (including velocity and pressure) normal to those boundary faces are zero.

The SST k-ω model of RANS method is applied to perform CFD simulation, in which the finite volume method and the second-order upwind scheme for spatial discretization are used and the SIMPLEC method is adopted to solve velocity and pressure simultaneously. The momentum equation, turbulent kinetic energy equation and specific dissipation rate equation are all discretized by the second-order upwind scheme. The simulation is continued until the residuals of all variables in the discrete equation are less than 10^{-3} accuracy and reaches steady state. In addition, velocity values at some locations near the mountain are also monitored until the velocity values do not change with iteration.

2.3 Simulation conditions

The wind field simulations over complex terrain around the SHW station are carried out for 16 inflow wind directions at a uniform interval 22.5° (clockwise positive from the north), which are consistent with the following wind tunnel test. The computational domains of 16 inflow wind directions can be achieved by rotating the complex topography around the SHW station shown in Fig. 6 with unchanging grid scheme and grid quality. In addition, after considering the topography distribution around the SHW station, the types of the topography around the SHW station are classified into sea fetch, land fetch and sea-land fetch. Sea fetch and land fetch are the cases for the inflow wind directions from 270° to 360° and 135° to 247.5° respectively, the other inflow wind directions belong to the sea-land fetch.

3. Wind field simulation over flat terrain

Before assessing wind field over complex terrain, the numerical simulation of wind field over a flat terrain domain is carried out to ascertain there is no substantial change in the prescribed inflow profiles. The dimensions of the flat terrain domain are the same as the computational domain of the 3-D complex terrain model.

Table 2 Errors of mean wind speed and turbulent kinetic energy between the inlet position and 11580 m position away from the inlet

Height	Inlet position		11580 m position		Error analysis	
z (m)	v (m/s)	k (m^2s^{-2})	v (m/s)	k (m^2s^{-2})	v (%)	k (%)
0	0.00	1.02	0.00	0.94	0.00	7.69
5	6.00	1.01	5.34	0.98	10.93	2.71
10	6.51	0.99	6.18	0.99	5.17	0.07
20	7.04	0.97	6.89	0.95	2.01	2.48
50	7.77	0.95	7.74	0.93	0.39	1.88
100	8.38	0.93	8.38	0.93	0.00	0.78
200	9.03	0.91	9.02	0.92	0.02	0.46
300	9.43	0.90	9.42	0.91	0.09	1.06
500	9.96	0.88	9.95	0.89	0.11	1.31
1000	10.73	0.86	10.72	0.86	0.06	0.76
2000	11.56	0.83	11.56	0.83	0.00	0.30
3000	12.08	0.81	12.08	0.81	0.05	0.13
4000	12.45	0.79	12.44	0.79	0.12	0.76
5000	12.73	12.73	12.58	12.58	1.18	1.18

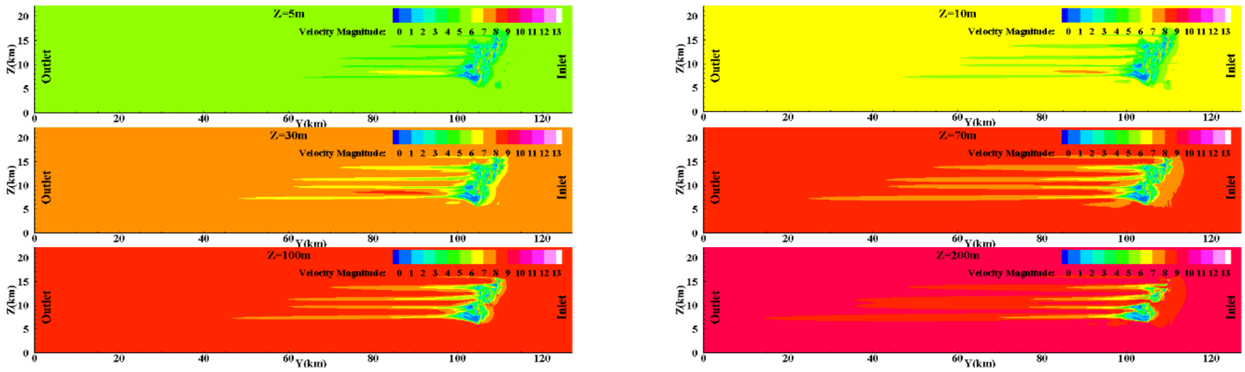

Fig. 10 Wind speed contours at different heights for 0° inflow wind direction

Fig. 9 shows the mean wind speed and turbulent kinetic energy profiles at 3000 m, 6000 m, 9000 m and 11580 m away from flow inlet boundary. It should be noted that the distance from the inlet boundary to the complex terrain edge in flow direction was 11580 m. Error analysis of the mean wind speed and the turbulent kinetic energy profiles between the inflow position and the 11580 m position away from the inflow position is shown in Table 2. The maximum mean wind speed and turbulent kinetic energy errors occur at 5 m height with values about 10.93% and 7.69%, respectively. These errors are caused by the non-slip wall boundary of the bottom in the computational domain. The mean errors of mean wind speed and turbulent kinetic energy are only about 1.44% and 1.54%, respectively. In summary, the simulated wind field over empty domain can be deemed as relatively horizontally homogenous and the equilibrium atmospheric boundary layer conditions derived from SST k-ω model can be used to simulate the wind field over complex terrain around the SHW station.

4. Wind field simulations over complex terrain

For wind field over complex terrain under 0° inflow wind direction, contours of wind speed at 5 m, 10 m, 30 m, 70 m, 100 m and 200 m heights are shown in Fig. 10, in which the wind flows from the right of the computational domain. It can be known that the inlet and outlet boundaries have enough distance away from the complex terrain and the wind fields are fully developed before reaching and after passing the complex terrain. The wake flows of the wind field dissipate completely and do not have any adverse effect near the outlet boundary of the computational domain at different heights. The side and top boundaries also have enough distance away from the complex terrain and have no effect on the flow field over complex terrain. In summary, the wind filed over complex terrain can be deemed as fully development in the present CFD simulation. This conclusion can also be obtained for wind fields over complex terrain under all other inflow wind directions.

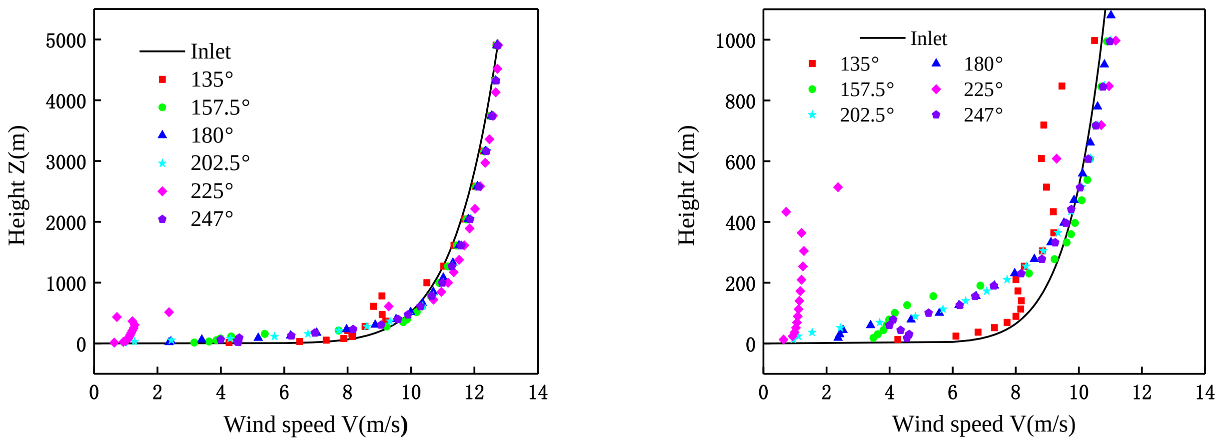

(a) Full height (b) Below 1000 m height

Fig. 11 Mean wind speed profiles for land fetch

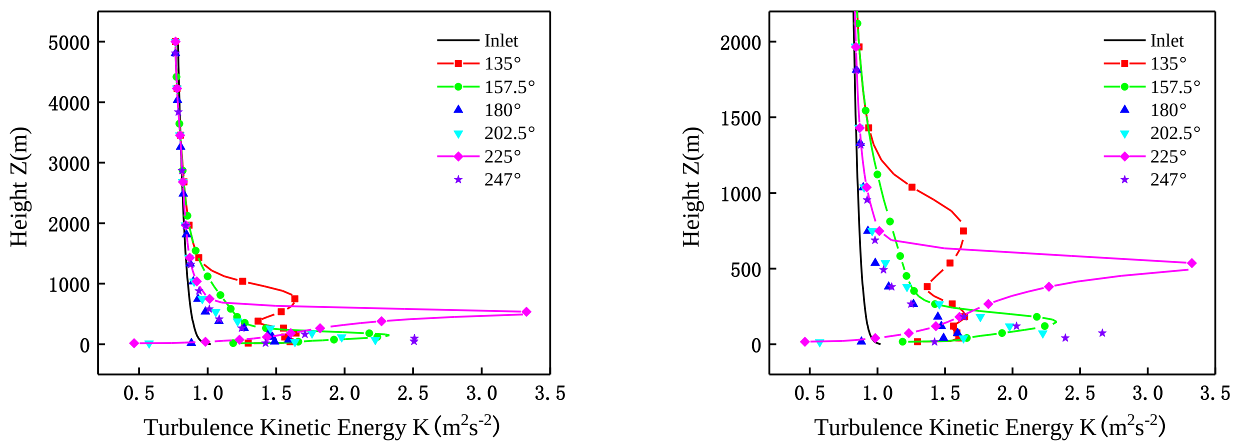

(a) Full height (b) Below 2000 m height

Fig. 12 Turbulent kinetic energy profiles for land fetch

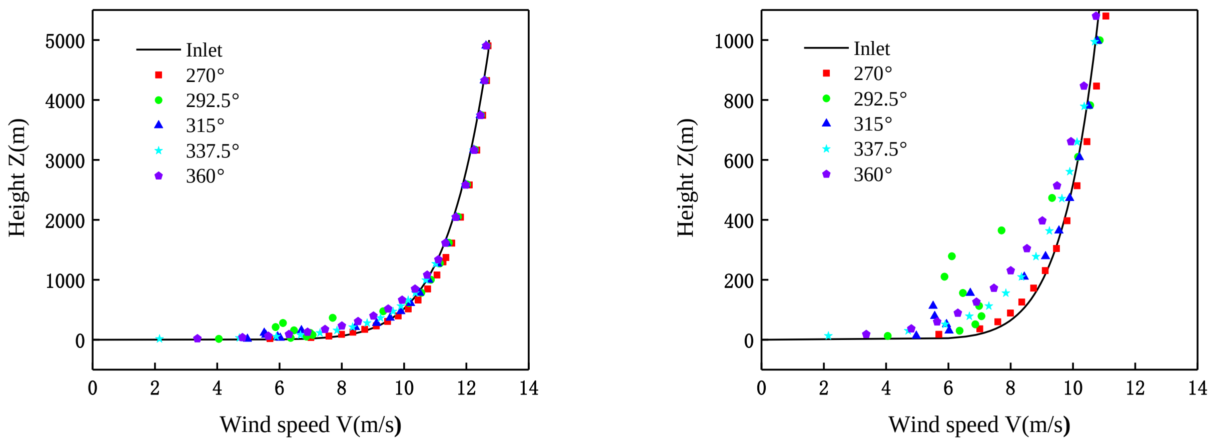

(a) Full height (b) Below 1000 m height

Fig. 13 Mean wind speed profiles for sea fetch

Mean wind speed and turbulent kinetic energy profiles at the SHW station for different fetches are shown in 11-16. The influence of complex terrain on the mean wind speeds and turbulent kinetic energies near ground surface varies with inflow wind direction. It should be emphasized that, the complex terrain has obvious influence on the wind field from 225° inflow wind direction which belongs to the land fetch. The downwind cross-section flow fields over complex terrain along the SHW station for 225° inflow wind direction are shown in Fig. 17. It can be seen from

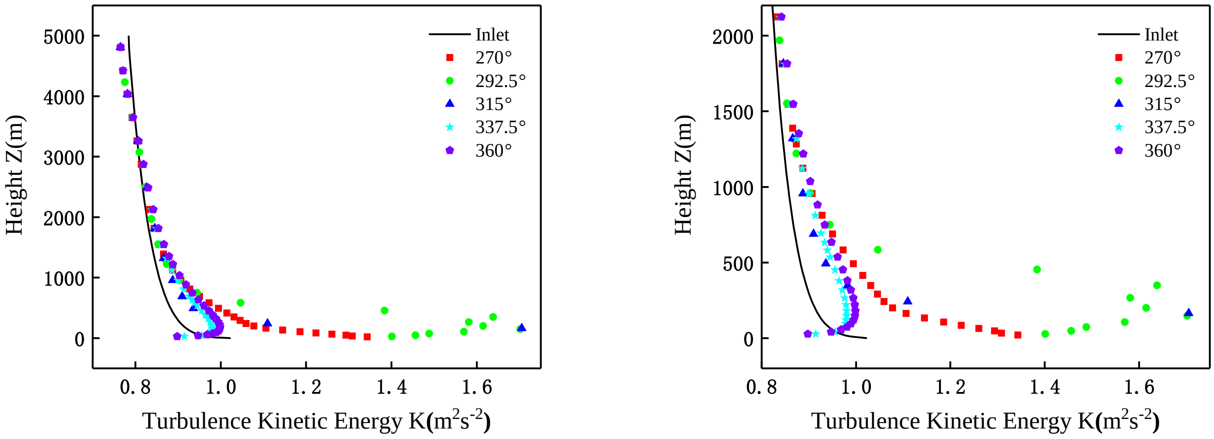

(a) Full height (b) Below 2000 m height

Fig. 14 Turbulent kinetic energy profiles for sea fetch

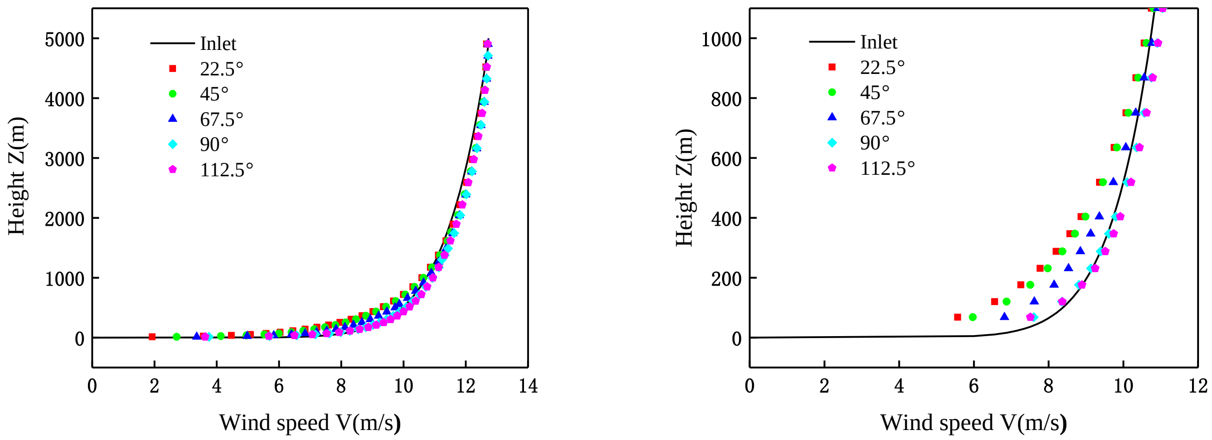

(a) Full height (b) Below 1000 m height

Fig. 15 Mean wind speed profiles for sea-land fetch

Figs. 11 and 12 that the mean wind speed is reduced and the turbulent kinetic energy is increased significantly near the ground surface. The reason is that the station is located at the backflow area and is affected obviously by the terrain. In addition, it can be seen from Figs. 13 and 14 that the mean wind speed and turbulent kinetic energy near ground surface at the SHW station for 292.5^{o} inflow wind direction are also reduced or increased significantly. The downwind cross-section flow fields for this inflow wind direction are shown in Fig. 19. The reason for this inflow wind direction is that the SHW station is located at a leeward side of the flow field and is hindered by the highest mountain of the complex terrain.

5. Results comparison

5.1 Wind tunnel test data

A wind tunnel test is carried out to simulate the wind field over complex terrain in the wind tunnel laboratory at City University of Hong Kong (Tse *et al.* 2014). The topography around the SHW station within 5 km are modeled at a geometric scale 1:4000 which is shown in Fig. 18. Wind speeds at 14 discrete heights above the SHW station were extracted and the elevations of 14 heights were 68 m, 120 m, 176 m, 231 m, 288 m, 347 m, 404 m, 519 m, 635 m, 751 m, 868 m, 984 m, 1100 m, 1216m, which are used to compare with the numerical results of this study.

5.2 Field measurement data

The Hong Kong Observatory had set up more than 40 observation stations to measure wind speeds and directions with Doppler SODARs and wind profilers. Hourly mean wind speed profiles at the SHW station were derived from the field measurement data during the passages of several typhoons from 2007 to 2009, which are used in the validation of the numerical simulation results of this paper. Detail information on these field measurement data can be found in Tse *et al*. (2014).

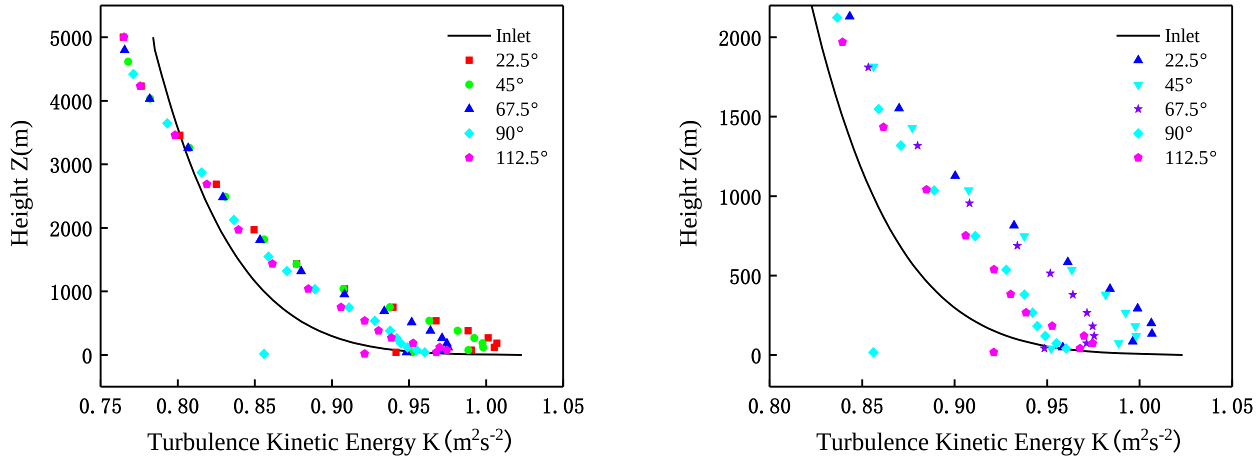

(a) Full height (b) Below 2000 m height

Fig. 16 Turbulent kinetic energy profiles for sea-land fetch

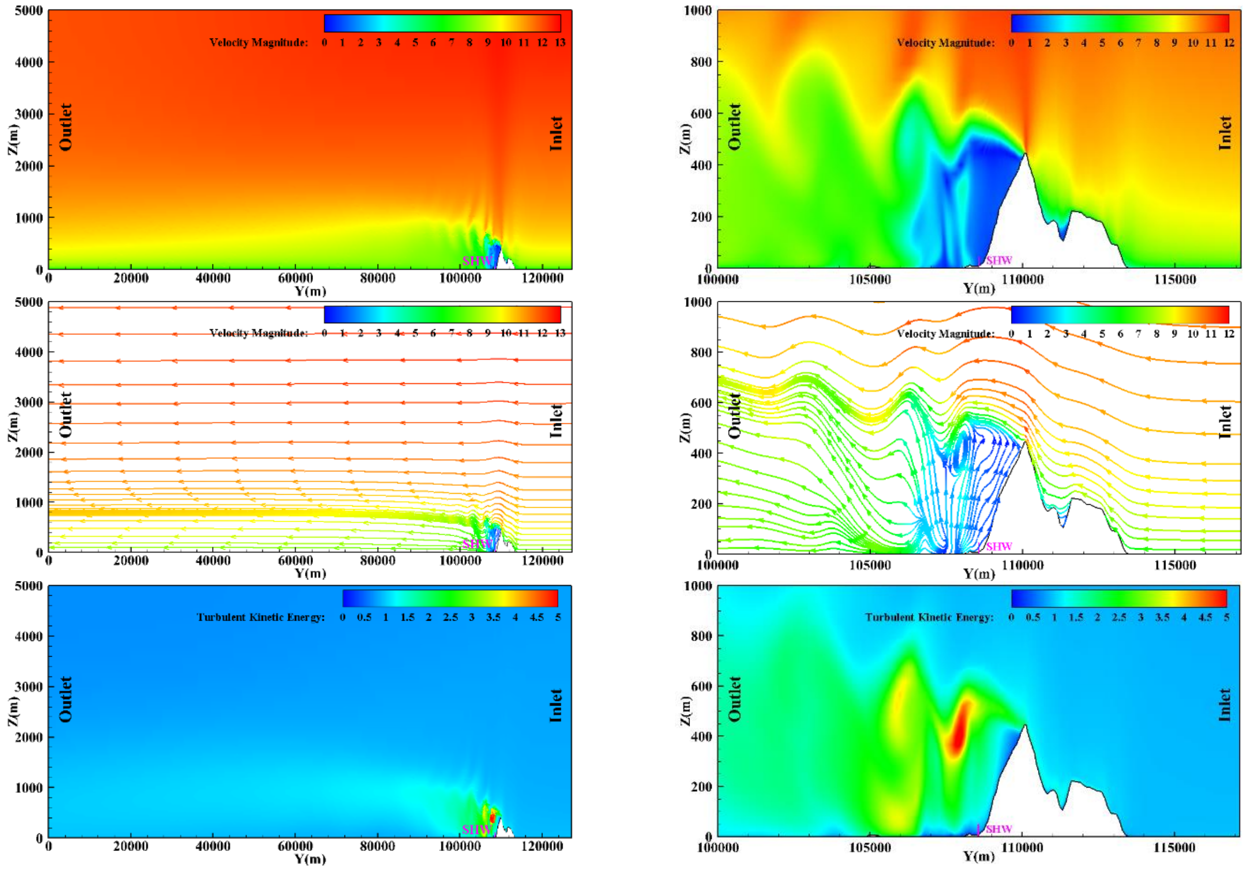

(a) Overall (b) Local

Fig. 17 Streamlines and contours of the mean velocity and turbulent kinetic energy along the SHW station for 225° inflow wind direction

5.3 Comparison and discussion

Although all data for the comparison are available (including field measurement data, wind tunnel test, and numerical results), these results cannot be compared directly since the wind tunnel test provides the mean wind speed profile shape but not the actual wind speed. To solve this problem, two methods are used in the following comparisons

Fig. 18 Wind tunnel test model at 0° wind direction

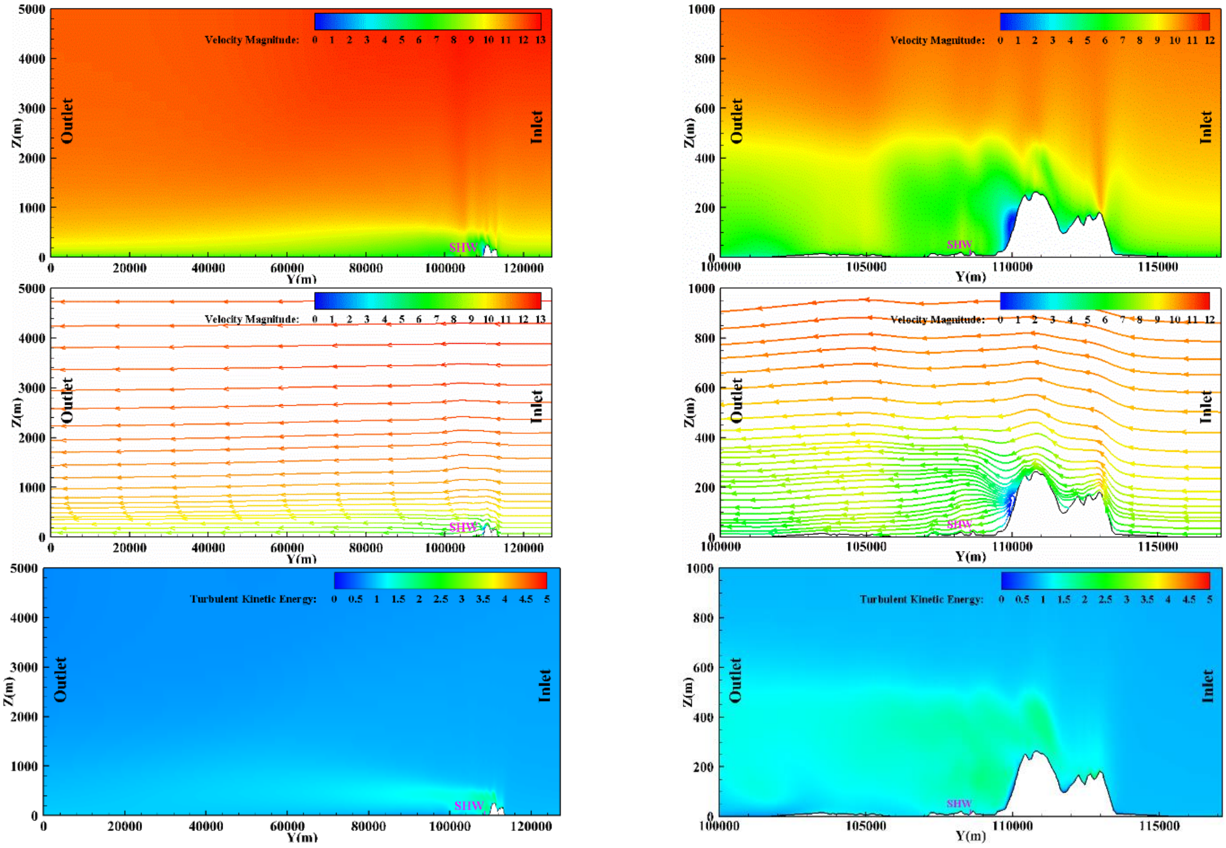

(a) Overall (b) Local

Fig. 19 Streamlines and contours of the mean velocity and turbulent kinetic energy along the SHW station for 292.5° inflow wind direction

(1) Comparison of normalized mean wind speed profiles: The mean wind speed profiles for each fetch is obtained by averaging the mean wind speed profiles for all inflow wind directions in corresponding fetch and the mean value of the mean wind speed for each fetch can be obtained by averaging mean wind speeds taken at 14 discrete heights. Then, the normalized mean wind speed profiles for each fetch can be obtained by dividing the mean wind speed profile with the mean value of mean wind speed in the fetch. Using the same way shown above, the normalized mean wind speed profiles for field measurement, wind tunnel test and numerical simulation can be obtained and compared.

(2) Comparison of amplified mean wind speed profiles: The normalized mean wind speed profiles of field measurement, wind tunnel test and numerical simulation are amplified by using the mean value of mean wind speed obtained from the numerical results and all amplified mean wind speed profiles are compared with each other.

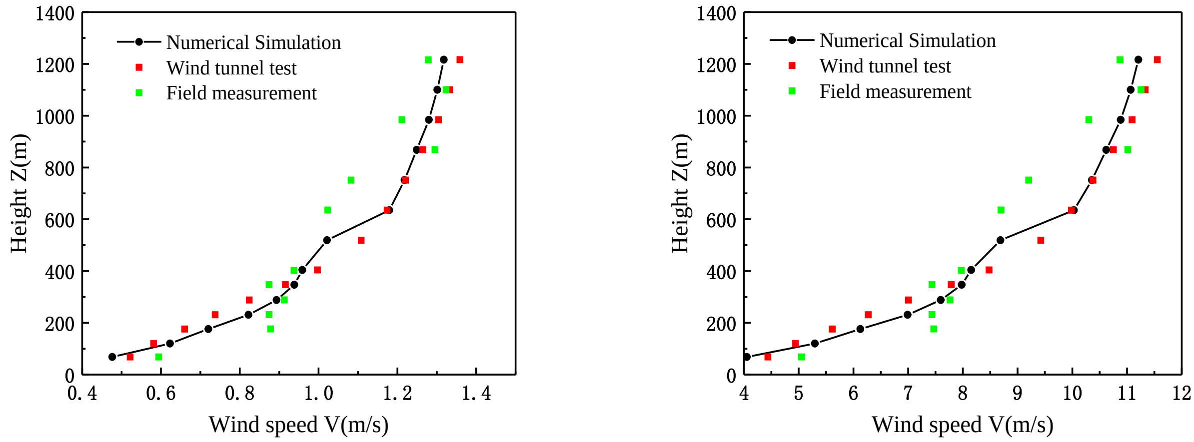

(a) Normalized (b) Amplified

Fig. 20 Comparison of mean wind speed profiles for the land fetch

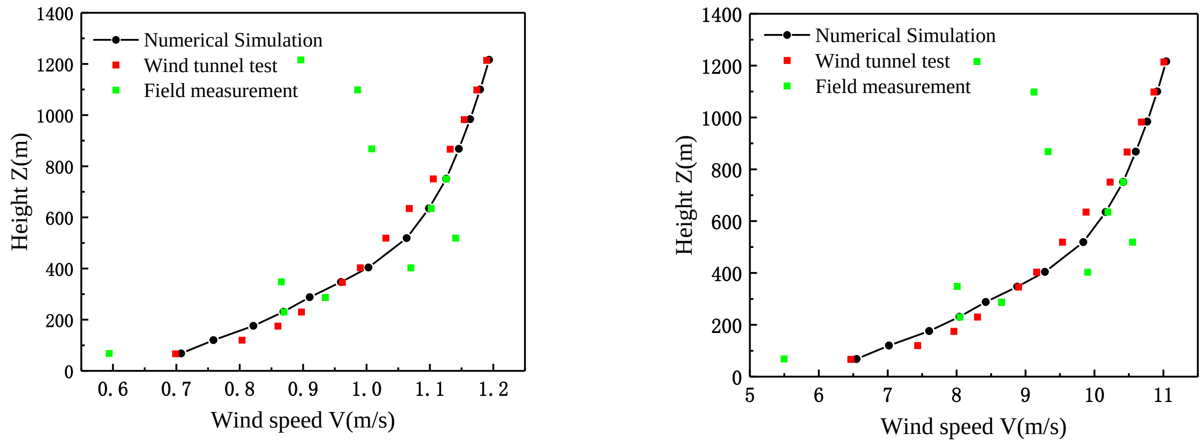

(a) Normalized (b) Amplified

Fig. 21 Comparison of mean wind speed profiles for the sea fetch

Comparisons of the normalized and amplified mean wind speed profiles for the land and sea fetches are shown in Figs. 20-21, respectively. For the land fetch, errors of mean wind speeds at 14 discrete heights between numerical results and field measurement results or wind tunnel test results for this fetch are shown in Table 3. Maximum and mean errors between numerical results and wind tunnel test results are 10.27% and 4.77%, respectively. Maximum and mean errors between numerical results and field measurement data are 18.12% and 8.6%, respectively. The results show that the numerical simulation give much closer results with the wind tunnel test than the field measurement data. Since the turbulence model used in numerical simulation is semi-theoretical model and some parameters used in the model are determined using the experiment results, which doesn't meet the requirement of engineering application. The expanded topography is obtained by using only the selected complex terrain around the SHW station, which is not consistent with the actual complex terrain. All these reasons will affect the wind field simulation over complex terrain and bring errors of numerical results.

Therefore, the numerical results of wind field over complex terrain with the present CFD simulation method can be deemed as satisfactory. The same conclusion can also be obtained for sea fetch. Errors of mean wind speeds at 14 discrete heights between numerical results and field measurement results or wind tunnel test results for sea fetch are shown in Table 4. Maximum and mean errors between numerical results and wind tunnel test results are 5.66% and 2.09%, respectively. Maximum and mean errors between numerical results and wind tunnel test results are 25.51% and 9.3%, respectively. In this fetch, the SHW station often locates at the windward field and the complex terrain has small effect on the mean wind speeds. Thus, the simulation results give much closer values with the field measurement data and the wind tunnel test results for sea fetch compared with the land fetch. It should be noted that, large errors can be found between the numerical results and field measurement data exceeding 800 m height. This is because that the super-gradient phenomenon of typhoon occurs onward this height sometimes for field measurement data (He *et al.* 2016), which cannot be depicted by the numerical

Table 3 Errors of mean wind speed profiles for the land fetch (NS: Numerical simulation; WT: Wind Tunnel; FM: Field Measurement)

Height (m)	NS (m/s)	WT (m/s)	FM (m/s)	Errors between NS and WT (%)	Errors between NS and FM (%)
68	4.05	4.44	4.95	9.54	18.12
120	5.30	4.94	6.06	6.68	12.63
176	6.13	5.61	7.30	8.37	16.04
231	6.99	6.27	7.28	10.27	3.97
288	7.60	7.01	7.59	7.75	0.15
347	7.98	7.79	7.26	2.40	9.88
404	8.15	8.48	7.79	4.01	4.66
519	8.69	9.42	8.16	8.48	6.41
635	10.03	9.98	8.50	0.46	17.95
751	10.36	10.38	8.99	0.20	15.24
868	10.62	10.75	10.75	1.23	1.18
984	10.89	11.09	10.06	1.90	8.21
1100	11.07	11.33	11.00	2.41	0.65
1216	11.21	11.55	10.61	3.09	5.61

Table 4 Errors of mean wind speed profiles for the sea fetch (NS: Numerical simulation; WT: Wind Tunnel; FM: Field Measurement)

Height (m)	NS(m/s)	WT(m/s)	FM(m/s)	Errors between NS and WT (%)	Errors between NS and FM (%)
68	6.55	6.49	5.46	0.84	16.64
120	7.02	7.44	6.26	5.66	10.75
176	7.60	7.97	7.13	4.61	6.16
231	8.04	8.31	7.98	3.24	0.81
288	8.42	8.66	8.53	2.71	1.27
347	8.88	8.91	7.98	0.30	10.18
404	9.28	9.17	9.81	1.26	5.67
519	9.84	9.54	10.46	3.17	6.26
635	10.16	9.88	10.10	2.87	0.59
751	10.42	10.23	10.32	1.84	0.97
868	10.60	10.48	9.24	1.17	12.81
984	10.77	10.68	9.14	0.77	15.09
1100	10.91	10.87	9.03	0.41	17.24
1216	11.04	11.00	8.23	0.39	25.51

simulation and the wind tunnel test in this study. The large errors between the numerical results and field measurement data are not found for the land fetch. This is because that the super-gradient height of typhoon in land fetch is much higher and exceeds 1200 m (He *et al.* 2016). In addition, wind field simulations over complex terrain around the SHW station were also performed by using the Weather Research and Forecast model (WRF) in Tse *et al.* (2014). The coarse resolution complex terrain model used in the WRF leads to an inaccurate simulation results of the low-level (<600 m) mean wind speeds. By contrast, since a high resolution and quality meshing complex terrain model is used in this study, the low-level height mean wind speeds can be predicted more satisfactorily by using the CFD simulation with RANS model, especially when the winds are coming from the land fetch.

6. Conclusions

Based on the digital terrain data around the SHW station, the complex terrain model with high-quality meshing for different inflow wind directions were built with Gambit and ICEM CFD software. The equilibrium atmospheric boundary layer conditions derived from SST *k-ω* model were validated and used to simulate the wind field over complex terrain around the SHW station. The numerical results were compared with wind tunnel test and field measurement data to verify the accuracy of the numerical simulation. The main conclusions are as follows:

- For the complex terrain model built with Gambit and ICEM CFD software, the minimum value of grid quality for the computational domain is 0.569, the maximum value is 1, of which 98.88% is greater than 0.9, which has good meshing quality and meets the calculation requirements.
- Based on the equilibrium atmospheric boundary layer conditions derived from SST k-ω model, the mean errors of mean wind speed and turbulent kinetic energy for the simulated wind field over empty domain are only about 1.44% and 1.54%, respectively. Thus, the equilibrium atmospheric boundary layer conditions can be used in wind field simulation over complex terrain.
- Although the terrain around the SHW station is complex, it can be concluded that the numerical results performed in this study can depict the wind field over complex terrain more satisfactorily. This can compensate the shortcoming of the WRF simulation perform by Tse *et al.* (2014).

In order to achieve the above conclusions, the following aspects are implemented in this study: (1) The original digital model needs to be expanded artificially into a flat terrain with zero elevation. (2) High quality computing domain mesh needs to be obtained. (3) The equilibrium atmospheric boundary layer simulation based on RANS turbulence model needs to be carried out, and the approximate inflow boundary conditions for wind field simulation over complex terrain should be established. The above research shows that, with the development of simulation technology, CFD simulation can provide credible and trustworthy results for wind field prediction over complex terrain and can provide effective guidance for wind resource assessment. At the same time, it should be realized that the wind field simulation over complex terrains still faces more serious challenges: (1) The existing boundary conditions for numerical simulations are ideal exponential or logarithmic wind velocity profiles. However, due to the limited scope of the concerned complex terrain, it is clearly not appropriate to use the above-mentioned conventional wind profile as an inlet boundary condition. (2) More disaster weather conditions such as typhoon and thunderstorm endanger the safety of building structures and it is more realistic to carry out wind field simulation over complex terrain under extreme weather conditions.

Acknowledgments

The work described in this paper was financially funded by National Natural Science Foundation of China (Project No: 51408174), Key University Science Research Project of Anhui Province (Project No: KJ2016A294), and the Fundamental Research Funds for the Central Universities (Project No: JZ2017YYPY0262). Any opinions and conclusions presented in this paper are entirely those of the authors.

References

Abdi, D.S. and Bitsuamlak, G.T. (2014), "Wind flow simulations on idealized and real complex terrain using various turbulence models", *Adv. Eng. Softw.*, **75**, 30-41.

Bitsuamlak, G.T., Stathopoulos, T. and Bédard, C. (2004), "Numerical evaluation of wind flow over complex terrain: Review", *Aerosp. Eng.*, **17**(4), 135-145.

Blocken, B., van der Hout, A., Dekker, J. and Weiler, O. (2015), "Cfd simulation of wind flow over natural complex terrain: Case study with validation by field measurements for ria de ferrol, galicia, spain", *J. Wind Eng. Ind. Aerod.*, **147**, 43-57.

Burlando, M., Carassale, L., Georgieva, E., Ratto, C.F. and Solari, G. (2007), "A simple and efficient procedure for the numerical simulation of wind fields in complex terrain", *Bound.- Lay. Meteorol.*, **125**(3), 417-439.

Castellani, F., Astolfi, D., Mana, M., Piccioni, E., Becchetti, M. and Terzi, L. (2017), "Investigation of terrain and wake effects on the performance of wind farms in complex terrain using numerical and experimental data", *Wind Energy*, **20**(7), 1277-1289.

Chaudhari, A., Vuorinen, V., Hämäläinen, J. and Hellsten, A. (2017), "Large-eddy simulations for hill terrains: Validation with wind-tunnel and field measurements", *Comput. Appl. Math.*, **37**(1), 1-22.

Conan, B., Chaudhari, A., Aubrun, S., van Beeck, J., Hämäläinen, J. and Hellsten, A. (2015), "Experimental and numerical modelling of flow over complex terrain: The bolund hill", *Bound. – Lay. Meteorol.*, **158**(2), 183-208.

Dhunny, A.Z., Lollchund, M.R. and Rughooputh, S.D.D.V. (2017), "Wind energy evaluation for a highly complex terrain using computational fluid dynamics (cfd)", *Renew. Energy*, **101**, 1-9.

Garcia, M.J. and Boulanger, P. (2006), "Low altitude wind simulation over mount saint helens using nasa srtm digital terrain model", *Proceedings of the International Symposium on 3d Data Processing, Visualization, and Transmission*, Chapel Hill, NC, USA, June.

He, Y.C., Chan, P.W. and Li, Q.S. (2016), "Observations of vertical wind profiles of tropical cyclones at coastal areas", *J. Wind Eng. Ind. Aerod.*, **152,** 1-14.

Hui, D.K., Kwok, K.C., Hitchcock, P.A. and Fok, C. (2006), "A comparison between computational fluid dynamics (cfd) analysis and wind tunnel observations on flow above a complex terrain", *Proceedings of the 4th International Symposium on Computational Wind Engineering (CWE2006)*, Yokohama, Japan, July.

Hussein, A.S. and El-Shishiny, H. (2009), "Influences of wind flow over heritage sites: A case study of the wind environment over the giza plateau in egypt", *Environ. Modell. Softw.*, **24**(3), 389-410.

Ishihara, T. (2003), "A nonlinear wind prediction model mascot: Development and application(numerical prediction technique of airflow over complex terrain)", *Japan Soc. Fluid Mech.*, **22**, 387-396.

Kamio, T., Iida, M. and Arakawa, C. (2014), "Analysis on turbulent flows using large-eddy simulation on the seaside complex terrain", *Physics: Conference Series*, **555**, 012058.

Kikuchi, Y. and Ishihara, T. (2012), "A study of topographic multiplier considering the effect of complex terrains and tropical cyclones", *J. Wind Eng. Ind. Aerod.*, **104-106**, 558-564.

Kim, H.G., Patel, V. and Lee, C.M. (2000), "Numerical simulation of wind flow over hilly terrain", *J. Wind Eng. Ind. Aerod.*, **87**(1), 45-60.

Kuo, J.Y.J., Romero, D.A., Beck, J.C. and Amon, C.H. (2016), "Wind farm layout optimization on complex terrains – integrating a cfd wake model with mixed-integer programming", *Appl. Energy*, **178,** 404-414.

Lee, M., Lee, S.H., Hur, N. and Choi, C.K. (2010), "A numerical simulation of flow field in a wind farm on complex terrain", *Wind Struct.*, **13**(4), 375-383.

Li, B., Zuo, L., Li, J., Wang, P., Liang, H. and Huang, Q. (2016), "Simulation-based micro-site selection for wind farm in complex terrain", *Proceedings of the International Conference on Smart Grid and Clean Energy Technologies*, Chengdu, China, October.

Li, C., Zhou, S., Xiao, Y., Huang, Q., Li, L. and Chan, P.W. (2017), "Effects of inflow conditions on mountainous/urban wind environment simulation", *Build. Simul.*, **10**(4), 573-588.

Li, J., Hu, F., Cheng, X. and Zhu, R. (2013), "Application of cfd on the simulation of the wind energy over complex terrain", *Acta Energiae Solaris Sinica*, **34**(7), 1250-1256.

Li, X., Liu, C., Leung, D. and Lam, K. (2006), "Recent progress in cfd modelling of wind field and pollutant transport in street canyons", *Atmos. Environ.*, **40**(29), 5640-5658.

Liu, Z., Ishihara, T., He, X. and Niu, H. (2016), "Les study on the turbulent flow fields over complex terrain covered by vegetation canopy", *J. Wind Eng. Ind. Aerod.*, **155**, 60-73.

Ma, Y. and Liu, H. (2017), "Large-eddy simulations of atmospheric flows over complex terrain using the immersed-boundary method in the weather research and forecasting model", *Bound. – Lay. Meteorol.*, **165**(3), 421-445.

Marjanovic, N., Wharton, S. and Chow, F.K. (2014), "Investigation of model parameters for high-resolution wind energy forecasting: Case studies over simple and complex terrain", *J. Wind Eng. Ind. Aerod.*, **134**, 10-24.

Meo, M., Tammaro, U. and Capuano, P. (2008), "Influence of topography on ground deformation at mt. Vesuvius (italy) by finite element modelling", *Nonlinear Mech.*, **43**(3), 178-186.

Murali, A. and Rajagopalan, R. (2017), "Numerical simulation of multiple interacting wind turbines on a complex terrain", *J. Wind Eng. Ind. Aerod.*, **162,** 57-72.

Palma, J.M.L.M., Castro, F.A., Ribeiro, L.F., Rodrigues, A.H. and Pinto, A.P. (2008), "Linear and nonlinear models in wind resource assessment and wind turbine micro-siting in complex terrain", *J. Wind Eng. Ind. Aerod.*, **96**(12), 2308-2326.

Petry, A.P., Loredo-Souza, A.M., Filho, D.G.R.D.F., Mattuella, J.M.L. and Oliveira, M.G.K. (2012), "Wind tunnel and CFD analysis of wind flow over a complex terrain-Dewek 2012", *Proceedings of the 12th German Wind Energy Conference-Dewek,* Bremen, Germany, November.

Prospathopoulos, J.M., Politis, E.S. and Chaviaropoulos, P.K. (2012), "Application of a 3d rans solver on the complex hill of bolund and assessment of the wind flow predictions", *J. Wind Eng. Ind. Aerod.*, **107-108,** 149-159.

Risan, A., Lund, J.A., Chang, C.Y. and Sætran, L. (2018), "Wind in complex terrain-lidar measurements for evaluation of CFD simulations", *Remote Sens.*, **10**(1), 59.

Salmon, J., Teunissen, H., Mickle, R. and Taylor, P. (1988), "The kettles hill project: Field observations, wind-tunnel simulations and numerical model predictions for flow over a low hill", *Bound.- Lay. Meteorol.*, **43**(4), 309-343.

Scargiali, F., Di Rienzo, E., Ciofalo, M., Grisafi, F. and Brucato, A. (2005), "Heavy gas dispersion modelling over a topographically complex mesoscale: A cfd based approach", *Process Saf. Environ. Protection*, **83**(3), 242-256.

Sherman, C.A. (1978), "A mass-consistent model for wind fields over complex terrain", *J. Appl. Meteorol.*, **17**(3), 312-318.

Shu, Z. R., Li, Q. S. and He, Y. C. (2017), "Vertical wind profiles for typhoon, monsoon and thunderstorm winds", *J. Wind Eng. Ind. Aerod.*, **168**, 190-199.

Tse, K.T., Li, S.W. and Fung, J.C.H. (2014), "A comparative study of typhoon wind profiles derived from field measurements, meso-scale numerical simulations, and wind tunnel physical modeling", *J. Wind Eng. Ind. Aerod.*, **131**, 46-58.

Uchida, T. and Ohya, Y. (1999), "Numerical simulation of atmospheric flow over complex terrain", *J. Wind Eng. Ind. Aerod.*, **81**(1), 283-293.

Uchida, T. and Ohya, Y. (2003), "Large-eddy simulation of turbulent airflow over complex terrain", *J. Wind Eng. Ind. Aerod.*, **91**, 219-229.

Uchida, T. and Ohya, Y. (2008), "Micro-siting technique for wind turbine generators by using large-eddy simulation", *J. Wind Eng. Ind. Aerod.*, **96**(10), 2121-2138.

Van Hooff, T. and Blocken, B. (2010), "Coupled urban wind flow and indoor natural ventilation modelling on a high-resolution grid: A case study for the amsterdam arena stadium", *Environ. Model. Softw.*, **25**(1), 51-65.

Weng, W., Taylor, P.A. and Walmsley, J.L. (2000), "Guidelines for air flow over complex terrain: Model developments", *J. Wind Eng. Ind. Aerod.*, **86**, 169-186.

Yamaguchi, A., Ishihara, T. and Fujino, Y. (2006), "Numerical modeling of local wind focusing on computational domain setting and boundary treatments", *JWE*, **108**, 185-188.

AD